Effects of Precursor Concentration on the Structural, Optical and Electrical Properties of Nebulized Spray Pyrolysis SnS Thin Films

P. S. Satheeshkumar[1], J. Raj Mohamed[2], S. Palanichamy[3], L. Amalraj[4]

[1,3,4]PG & Research Department of Physics, V.H.N.S.N. College, Virudhunagar 626001, Tamilnadu, India

[2]PG & Research Department of Physics, H.H. The Rajah's College, Pudukkottai 622001, Tamilnadu, India

[1]pssatheesh@yahoo.com, [2]raj.shafraz@gmail.com, [3]nanopalani@gmail.com, [4]amalraj.raj1973@gmail.com

Abstract **-** At the substrate temperature of 300 °C thin films of tin sulphide (SnS) with different precursor concentrations have been prepared by the nebulized spray pyrolysis technique. The physical properties of the films were studied as a function of increase precursor concentration (up to 0.150 M). The films were characterized by different techniques to study their structural, optical and electrical properties. The X-ray diffraction analysis revealed that the films were polycrystalline in nature and having orthorhombic crystal structure with a preferred orientation in (111) direction. The crystalline quality and the preferential orientation of SnS films were improved at 0.125 M of concentration due to increase in precursor concentration. Optical measurements showed that the band gap values decreased from 2.24 eV to 1.81 eV with increase precursor concentration from 0.050 to 0.125 M. The better conductivity and mobility are noticed at m_c=0.125 M is explained by carrier concentration and crystallite. Better optical end electrical conductivity behaviour of SnS thin film sample suggests for solar cell applications.

Keywords **- SnS, Nebulized spray pyrolysis, Precursor concentration, Band gap, resistivity, activation energy.**

I. INTRODUCTION

Investigations on tin mono sulphide (SnS) semiconductor demonstrated that it has an optical energy band gap of ~1.3 eV **[1]**and exhibits high absorption coefficient (~10^5 cm^{-1}), which is greater than that of presently existing materials such as GaAs, CdTe **[2]**. This band gap is nearer to the optimum value of 1.4 eV for efficient absorption of electromagnetic radiation above the visible radiation. Its constituent elements such as 'Sn' and 'S' are abundant in nature, less toxic and available at low cost. In addition, it has shown high theoretical solar conversion efficiency (>24% **[3]**).These properties made SnS as one of the candidates for the fabrication of hetero-junction solar cells.

A thin film deposition technique that can be easily handled at low cost is needed for large-scale production of solar cells. The SnS thin films were prepared with different techniques such as vacuum evaporation **[4]**, RF-sputtering **[5]**, cathodic electrode position **[6]**, electrochemical deposition **[7]**, chemical vapour deposition **[8]** and spray pyrolysis**[9-12]**.

Among these, the spray pyrolysis technique is advantageous for large-scale production of thin films with variable film thicknesses. However, the reported investigations on sprayed SnS films in relation to their solar cell application are meager and it is therefore recognized that a detailed study on the physical characteristics of this material is very much essential to estimate its suitability for photovoltaic as well as optoelectronic device applications. Among these methods, even though the physical techniques deposit high quality and uniform thin films, they are comparably overpriced and extremely energy consuming. Nebulized spray technique (NSP) is a versatile, cost-effective, simple, time-saving and efficient way of depositing thin films at room atmosphere. For large area deposition this technique can be ascendable.

In the present investigation, the binary SnS thin films have been deposited on the micro glass substrate by NSP technique for different precursor concentration (m_c) from 0.050 M to 0.150 M. Structural, optical, morphological, elemental and electrical conductivity properties of nebulised spray deposited SnS thin films have been reported.

II. EXPERIMENTAL TECHNIQUE

A. Materials and Methods

High purity chemicals (> 99% purity) such as Tin chloride ($SnCl_2$) (Sigma-Aldridge) and thiourea ($CS(NH_2)_2$) (GR E Merck) were used for the preparation of SnS thin films as precursor without further purification. The precursor $SnCl_2$ and $CS(NH_2)_2$ were used as source materials of Sn and S ions respectively. To deposit SnS thin films micro glass slides have been used as substrates. In this work, the SnS thin films were deposited with different precursor concentration from 0.050 M to 0.150 M. The substrate temperature was constrained by an iron-constantan type thermocouple and kept constant as its optimized value of 300 ^oC. The oxygen carrier gas flow rate was maintained at 1 kg/cm^2 corresponding to an average pressure solution rate of 10 ml per 10 minutes. The precursor solution was held in the nebulizer unit, which is connected to an air compressor. The compressed air is transported by tubing and it stimulates the precursor solution through an "L" glass tube. The mist like tiny droplets of particles was carried to deposit onto the glass substrate kept in the uniform hot zone of the furnace, from the glass tube. After deposition, the films were allowed to cool at room temperature and then preserved them in desiccators.

B. Characterization Technique

The structural and chemical phases of the SnS films were ascertained over a 2θ range of 10 – 65^o by X-Pert Pro X-ray diffract meter (CuKα, λ=1.5405 Å). The optical properties using optical absorption spectrum were observed using UV-Vis-NIR double beam spectrophotometer (Hitachi U3410 model) over the wavelength range 300 – 1100 nm. Scanning electron microscope (SEM) was used to find the dispersion of particles, rough morphology and the particle size on the surface of the film. The surface morphology of the as-deposited SnS films was analysed by scanning electron microscope (SEM, Genesis model). The chemical composition of Sn and S was determined by energy dispersive analysis by X-rays (EDAX) on K and L lines.

The electrical conductivity of the as-deposited films was found by Hall Effect measurement system by ECOPIA-HMS 5000 model. With a stylus profile meter (Mitutoyo, SJ-301) the thickness of the SnS layers was determined.

III. RESULTS AND DISCUSSION

Various characterizing techniques are described for the as-deposited SnS thin films for different precursor concentration and the results for the corresponding films have been discussed.

A. Structural characterization

The X-ray diffraction pattern of SnS films of different precursor concentrations deposited at an optimized substrate temperature of 300 ^{o}C, are shown in Fig.1. The XRD measurement exposed that all the as grown film layers were polycrystalline in nature. While the films deposited at other precursor concentrations showed mixed phases such as Sn-O-S and $Sn_2S_3$with different structures. The phases identified in the films grown at m_c = 0.050 M are related to Sn-O-S. Whereas for concentrations m_c>0.050 M, Sn_2S_3phases is present along with SnS phase. The observed change in the formation of various phases with the change of m_c can be attributed to the variation of the composition in the films. At lower concentrations, due to less availability of sulphur, tin might react with atmospheric oxygen to obtain stabilised structure and forms phases belongs Sn-O-S complex. At higher concentrations, the presence of Sn_2S_3along with SnS phase might be due to either the availability of more sulphur or the lack of thermal energy for top clusters. A similar behaviour of the formation of different phases with the change of substrate temperature was reported by Lopez et al. and Koteeswara Reddy et al. **[13, 14]** for SnS films.

The films grown in the precursor concentration range, 0.050 ≤ m_c≤ 0.150 M showed only SnS phase with a strong (111) preferred orientation diffracted at 2θ is 31.72^{o}.The films exhibited an orthorhombic crystal structure with the lattice parameters, a = 0.431 nm, b = 1.119 nm and c = 0.398 nm. The evaluated inter-planar d-spacing and the lattice parameters are in good agreement with JCPDS files of SnS (JCPDS 39-0354).The other peaks observed in the XRD spectrum of films are (131) and (151)at 2θ values of 39.1^{o} and 51.4^{o}, respectively.

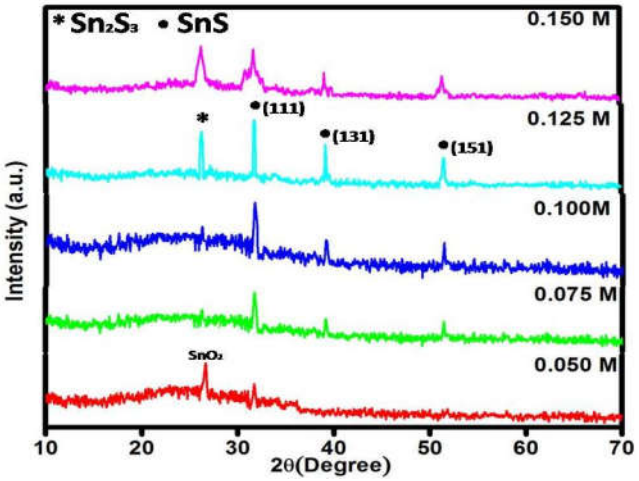

Fig.1 X-ray diffraction pattern of nebulized spray deposited SnSthin films at Different precursor concentration

Fig.2 shows the variation of thickness as a function of precursor concentrations from 0.050 M to 0.150 M. The film thickness increases from 284 to 378 nm when precursor concentration is increased from 0.050 M to 0.150 M. The preparative parameters as substrate temperature, deposition time, molarity ratio, compressed air etc. decide the growth and quality of the film.

According to Bauer **[15]**, there are two attainable mechanism of the orientation owing to nucleation and final growth, both of which effect from the nucleation at the film / substrate with the inclination of nuclei to work out a minimum free energy configuration. The final growth orientation results from the endurance of nuclei having an energetically unstable plane parallel to the substrate surface amidst randomly oriented nuclei due to their different growth rates. This means that the growth orientation is formulated into one crystallographic direction of the lowest surface energy. Then as the film grows with lower surface energy density, the grains became larger Thenceforth, with increasing molarity, the solution comprises more sulfur ions. As thickness reckons on the band gap of thin film deposition at higher molar concentrations are thicker as compared to films deposited at lower molar concentration. Since in thin films, the average crystallite size is proportional to thickness of films, the decrease in band gap with the increase in film thickness in this study indicates that there is no charge accumulation at grain boundaries in SnS thin films.

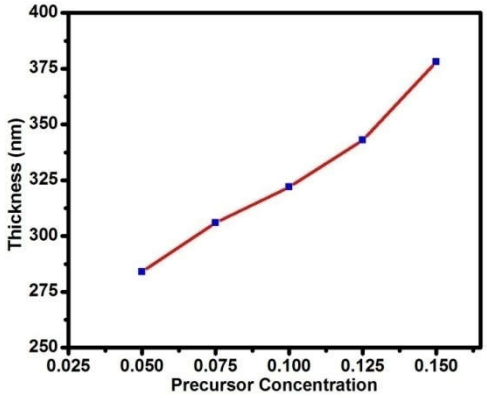

Fig.2 Variation of thickness of SnS thin films at different precursor concentration

In general, crystallite size and lattice strain regulate the Bragg peaks in different ways such as instrumental factors, the existence of defects to the ideal lattice, differences in strain in different grains and the crystalline size. Both these effects elevate the peak width and intensity and shift the Bragg peak (2θ) position consequently. It is much executable to divide the effects of size and strain. The size broadening is independent of the length of the reciprocal lattice vector (q) and strain broadening increases with increasing q values. There will be both size and strain broadening in most of the cases **[16]**.

The texture coefficient $T_{c(hkl)}$ of the SnS thin films **[17]** have been calculated from the XRD data using the relation

$$T_{c\,(hkl)} = \frac{I_0(hkl)}{I_s(hkl)} \left[\frac{1}{N} \sum_{i=1}^{n} \frac{I_0(hkl)}{I_s\,(hkl)} \right]^{-1} \qquad (1)$$

Where I_0 (hkl) is the observed intensity, I_s(hkl) is the standard intensity, T_c is the texture coefficient and N is the number of diffraction peaks. The preferred orientation of films can be confirmed by the higher value of texture coefficient. The increased number of grains along the plane associates the increase in preferred orientations **[18]**.

The dislocation density (δ) defined as length of dislocation lines per unit volume of the crystal using grain size values (D) has been calculated using the Williamson and Smallman's formula **[19]**

$$\delta = 1/D^2 \text{lines}/m^2 \quad (2)$$

The number of crystallites per unit area (N) of the samples was found using the relation **[20]**

$$N = t / D^3 \quad (3)$$

TABLE 1 exhibits crystallite size (D), dislocation density (δ), lattice strain (ε_s) and thickness (t) of SnS thin films with different precursor concentration from 0.050 M to 0.150 M. Fig.3 shows the variation in the crystallite size, strain and dislocation density of the films as a function of precursor concentration. The crystallite size is low at lower precursor concentration since the deposited atoms in lieu of incorporating to the neighbouring grains and increasing their size are condensed and stay stuck to the region to constitute small nuclei and clusters. At higher precursor concentration, a large crystallite size is noticed due to the increasing mobility of the surface of atoms and increasing cluster formation.

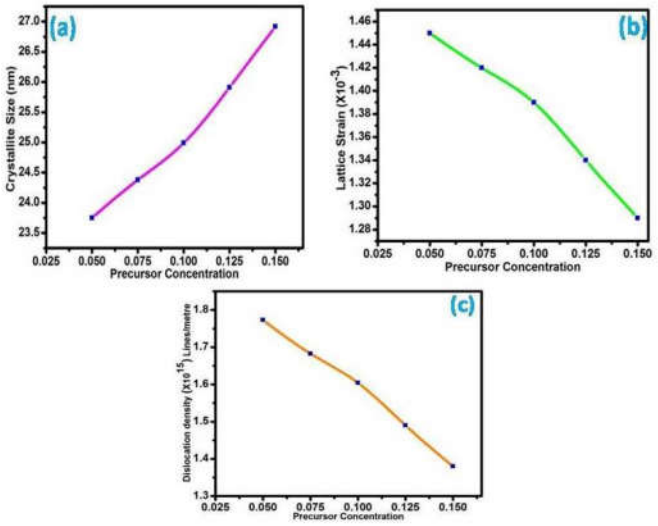

Fig. 3 The variation of structural parameters with different precursor concentration of SnS thin films (a) Crystallite size (b) Strain (c) Dislocation density

It is observed that the crystallite size increases and obtains a maximum value of 26.92 nm at m_c= 0.150 M whereas the decrease in lattice strain was observed by increasing the precursor concentration. Owing to the prevailing re-crystallization process in the SnS polycrystalline thin films surely, the lattice strain is decreased. The observed decrease of full width at half maximum (FWHM) of diffraction peaks with increase of precursor concentration can be attributed to the increase in crystallite size. The dislocation density of as prepared SnS films decreased as the precursor concentration increased. The minimum values of dislocation density are obtained for the film grown at the precursor concentration 0.150 M. This behaviour is explained by the change in grain size with precursor concentration. Indeed, the larger crystallites have a smaller surface to volume ratio, thus giving up a rise to the dislocation network. The number of crystallites per unit area (N) depends on the parameters like equidimensional crystallites and the degree of the agglomeration of the thin films. It is ascertained that the precursor concentration parameter increases as the number of crystallites decreases.

The average crystallite size calculated by Debye Scherrer formula for all the samples prepared at precursor concentration from 0.050 to 0.150 M was found to be increased from 23.75 to 26.92 nm.

TABLE 1

Structural analyses of SnS thin films deposited at different precursor concentration (m_c)

m_c (mole)	Texture coefficient	Crystallite size (nm)	Strain $x10^{-3}$	Dislocation density $x10^{15}$ (Lines/m^2)	No. of crystallites $x10^{16}$(m^2)	Thickness (nm)
0.050	1.2416	23.75	1.45	1.7731	2.1199	284
0.075	1.0391	24.38	1.42	1.6826	2.1116	306
0.100	1.0443	24.99	1.39	1.6041	2.0633	322
0.125	1.0109	25.91	1.34	1.4899	1. 9719	343
0.150	1.1081	26.92	1.29	1.3799	1.9376	378

B. Surface topology

Fig. 4 gives the SEM images that provide microscopic information of the surface topography. The effect of the precursor concentration on the surface morphology of the film is studied. The entire substrate surface is covered by the film, and pinholes are not found in the films. However, as the precursor concentration was increased, the distributions of grains have been reduced. At m_c = 0.050 M, the film is composed of nanometric round shaped grains yielding rise to a close-packed and adherent film while the film deposited at the precursor concentration m_c=0.075 M is composed by slightly bigger and irregular agglomerates. The surface of the as-deposited SnS thin film at m_c= 0.100 M shows a uniform granular structure with very well-defined grain boundaries and with some larger grains distributed on the film. The irregular round shaped grains of SnS crystallites have been found. The surface morphology of the film deposited at m_c = 0.125 M show a granular morphology. The grain size also increases, leading to coalescence of the grains. The film deposited at the precursor concentration of 0.150 M is composed of big nanometric round shaped grains with agglomerated morphology. The different sizes which are evidenced by the calculated grain size values.

C. Composition analysis

The characteristic EDX spectra of SnS thin films at different precursor concentrations from 0.025 M to 0.150 M are shown in Fig.5. It depicts the precise chemical composition of SnS thin films. It could be observed from the figure that the precursor concentration has a significant influence on the stoichiometric of the grown layers. The EDX spectra show well-defined peaks corresponding to Sn and S. The quantitative weight percentage of the compositional elements such as Sn and S from m_c= 0.025 M to 0.150 M are listed in TABLE 2.

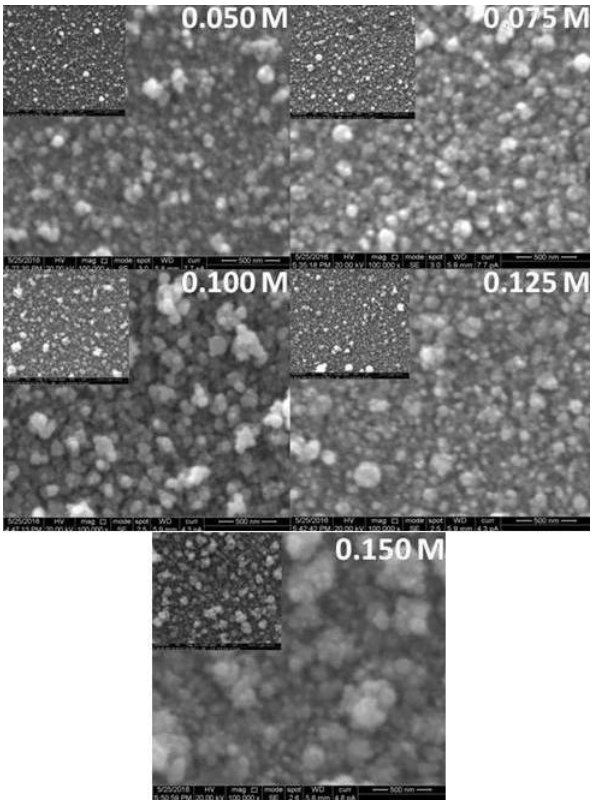

Fig .4 Scanning electron microscope (SEM) images of SnSthin films for different precursor concentration

TABLE 2

Variation of elemental analysis of SnS thin films at different precursor concentration

m_c (mole)	***Atomic percentage of the elements (%)***		***Sn/S ratio***
	Sn	***S***	
0.050	52.2	47.8	1.09
0.075	52.8	47.2	1.12
0.100	53.3	46.7	1.14
0.125	53.9	46.1	1.17
0.150	54.4	45.6	1.19

By increasing the precursor concentration the atomic percentage of tin is slightly increased from 52.2 to 54.4. Also Sn/S ratio in the layers increased with the increase of precursor concentration from 0.050 M to 0.150 M, reached a maximum at 0.125 M and 0.150 M (higher precursor concentration). The observed change in Sn/S ratio might be due to the deficiency of sulphur, which might be little above the detection limit of EDAX in the as-deposited films. EDX spectrum exhibits that the weight percentage is closely equal to their nominal stoichiometric within the experimental error.

D. Optical properties

Fig.6 shows the optical transmittance spectra of the as-deposited SnS films of different precursor concentrations. It can be ascertained that the transmittance of the as-deposited layers of precursor concentration 0.050 M is virtually similar as that of the films of m_c= 0.075 M (85-90%). While the precursor concentration at 0.100 M showed a significant change in the optical transmittance that decreased from 60% to 65% which may be due to the increase in the thickness of the films. The observed lower transmittance at the precursor concentration 0.100 M to 0.125 M could be due to the stoichiometric deviations and thickness. There is increase in optical transmittance from 75% to 80% of 0.150 M might be due to the decrease of residual defects and the increase of crystallite size **[21]**.

The optical energy band gap of the as-deposited thin films was measured using the relation given in equation.

$$(\alpha h\nu) = A\left(h\nu - E_g\right)^p \quad (4)$$

The optical energy band gap (E_g) of the as-deposited SnS thin films was found using $(\alpha h\nu)^2$ versus photon energy plots as shown in Fig.7. The direct optical band gaps of SnS thin films was found to be 2.24, 2.20, 2.01, 1.81 and 1.94 eV with increase in the precursor concentration from 0.050 M to 0.150 M. The direct band gap values of SnS thin films reported in the literatures extend from1.0 eV up to 1.45 eV **[22-31]**. Due to presence of SnS with Sn_2S_3 phases **[32]** there are wider band gaps. Typically, in polycrystalline semiconductors, the energy band gap can be impacted by the quantum size effect **[33]**, modification in the preferred orientation of the film **[34]**, disorder and dislocation of density at the grain boundaries **[35]**. The sharp reduction of energy band gap at higher precursor concentration could be owing to the constitution of localized states in the band gap region. These states might be elicited in the band gap on account of the structural disorder owing to the sulphur deficiency. The band structure to sledge is stimulated by the high concentration of impurity states, resulting in a prolonged tail extending into the energy band gap Furthermore; the energy band gap could also be influenced by the change of particle size with precursor concentration as it is in the nanometre range even though it is not close to the Bohr radius. Hence, in this study both the improvement in the particle size and the stoichiometric deviations could contribute to the decrease of energy band gap of the films with the increase in the precursor concentration.

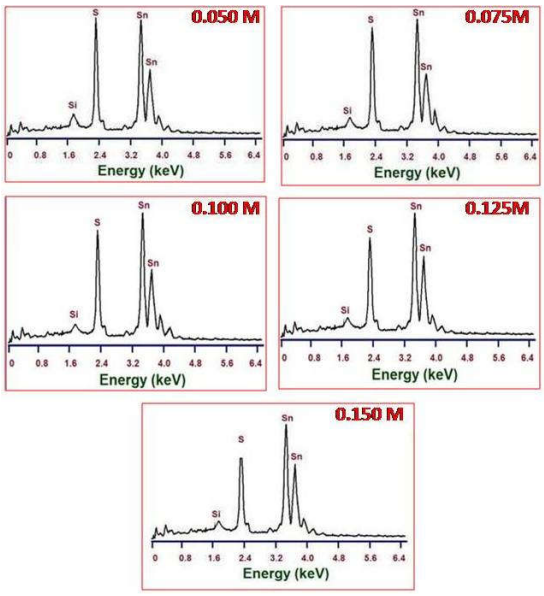

Fig.5 Energy dispersive X-ray (EDX) pictures of SnS thin film for different precursor concentration

E. Electrical properties

The electrical conductivity, resistivity, Hall coefficient, mobility and bulk carrier concentration of SnS thin films deposited at different precursor concentration were determined by Hall Effect measuring instrument and the corresponding values were listed in TABLE 3. The Hall coefficient values conform that the films had an n-type characteristic. The variation in the resistivity, carrier concentration and Hall mobility of the films as a function of precursor concentration is shown in Fig. 8. The resistivity of the as-deposited films decreases with increase precursor concentration from 0.050 M to 0.125 M. The lowest resistivity value was 0.73 Ωcm at the precursor concentration of 0.125 M. The decrease in resistivity may be attributed to the increase in crystallite size which leads to a decrement in the trapping states at grain boundary **[36]**. The grain boundary plays an important role between the crystallites and the carrier transport. It can act as a trap center in an incomplete atomic bonding, which depletes the free charge carriers and as a resultant, more number of free carriers become immobilized as trapping state increase**[37]**. The precursor concentration had increased to 0.150 M to exhibit p-type electrical conduction while the resistivity again increases to 12.95 Ωcm. Meanwhile, the conductivity of the films is increased with the increase in the precursor concentration. It is ascertained that for the films deposited at different precursor concentrations up to 0.125 M. The Hall mobility and bulk carrier concentration increases with increase in precursor concentration up to 0.125 M and decreases with the further increase in precursor concentration. The bulk carrier concentration and mobility of the SnS thin films increase with increasing precursor concentration up to 2.286 x 10^{18} cm^{-3} and 23.6 cm^2/Vs, respectively. As a result of reconstituting and the crystallinity prosperity of the material the mobility increases. The mobility values is closer to the values obtained by Ngamnit Wongcharoen et al. **[38]** for SnS thin films grown by vacuum thermal evaporation method. The results depicted in this work have presented the feasibility of using SnS thin films as absorber layers in cadmium free thin film solar cells.

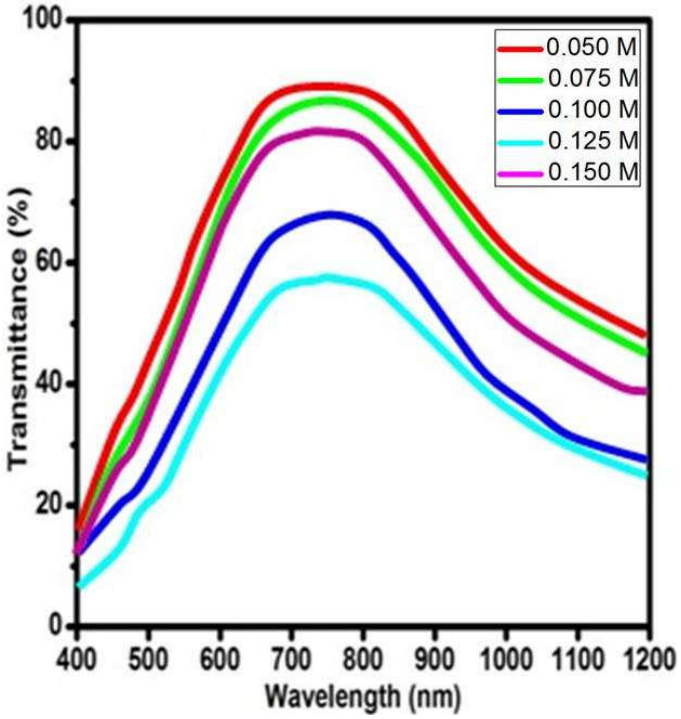

Fig. 6 Wavelength versus transmittance spectra of nebulized spray deposited SnS thin films

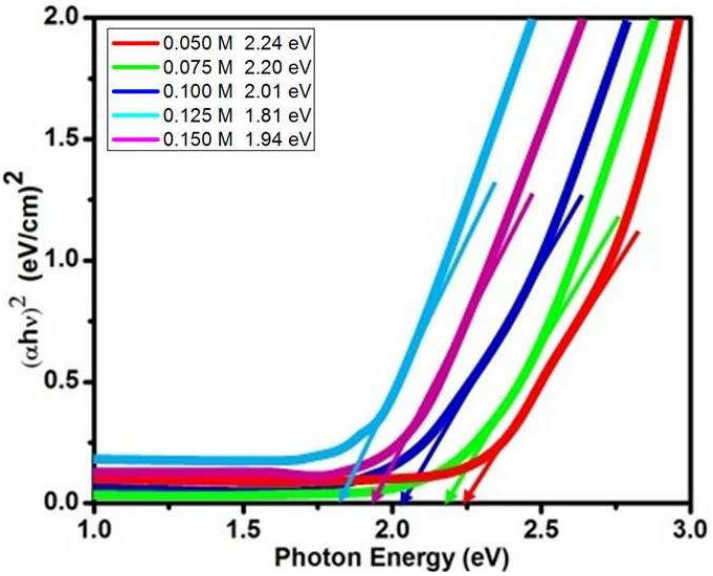

Fig.7 Plot of $(\alpha h\nu)^2$ versus Photon Energy for nebulized spray deposited SnS thin films for different precursor concentration

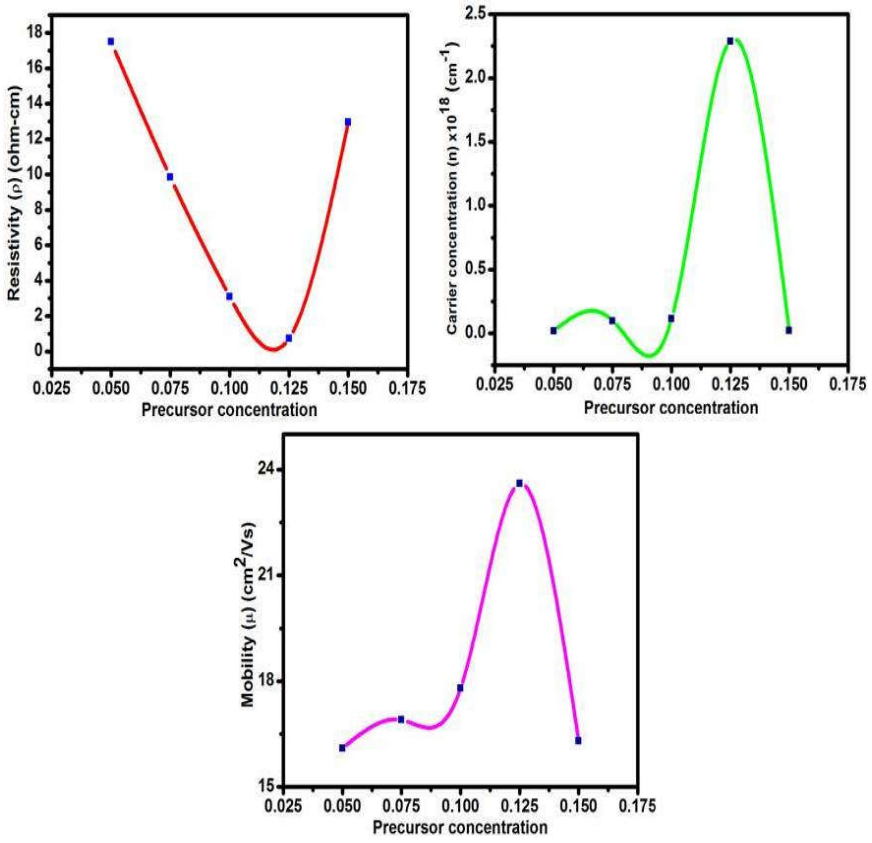

Fig.8 Variation of resistivity, carrier concentration and mobility of SnS thin films of different precursor concentration

The activation energy of the SnS thin films was calculated as a function of precursor concentration of tin species in the range of 0.050 M to 0.150 M by determining the resistivity of each sample at different temperatures and using the equation

$$\rho = \rho_0 exp^{(E_a/KT)} \quad (5)$$

The Arrhenius plot was drawn with these data as shown in Fig.9. The activation energy for SnS thin films were calculated as 0.43 eV, 0.37 eV, 0.27 eV, 0.12 eV, and 0.16 eV corresponding to 0.050 M, 0.075 M, 0.100 M, 0.125 M, and 0.150 M precursor concentrations, respectively. Juarez et al.

[39] also had reported the activation energy of 0.15 eV for mixture of SnS and Sn_2S_3 compounds were deposited with higher values of the relative concentration. The present result shows similar to the previous author **[39]**. It was found that the activation energy values decreases with increase in precursor concentration up to 0.125 M and then increases for the further increase in precursor concentrations. The decrease in activation energy with the increase in precursor concentration may be attributed to the change in the electronic structure corresponding to the increase in thickness values **[40]**. Similar activation energy value was reported by Lopez et al **[41]** of 0.54 eV for sprayed SnS films.

TABLE 3

Variation of optical and electrical properties of SnS thin films at different precursor concentration

m_c (mole)	***Band gap (eV)***	***Resistivity (Ωcm)***	***Carrier concentration (cm^{-3})***	***Mobility (cm^2/Vs)***	***Hall coefficient (cm^{-3}/C)***
0.050	2.24	17.50	$1.905x10^{16}$	16.1	$3.289x10^{2}$
0.075	2.20	9.85	$9.753x10^{16}$	16.9	$6.410x10^{1}$
0.100	2.01	3.10	$1.132x10^{17}$	17.8	$5.522x10^{1}$
0.125	1.81	0.73	$2.286x10^{18}$	23.6	$2.741x10^{0}$
0.150	1.94	12.95	$1.985x10^{16}$	16.3	$3.157x10^{2}$

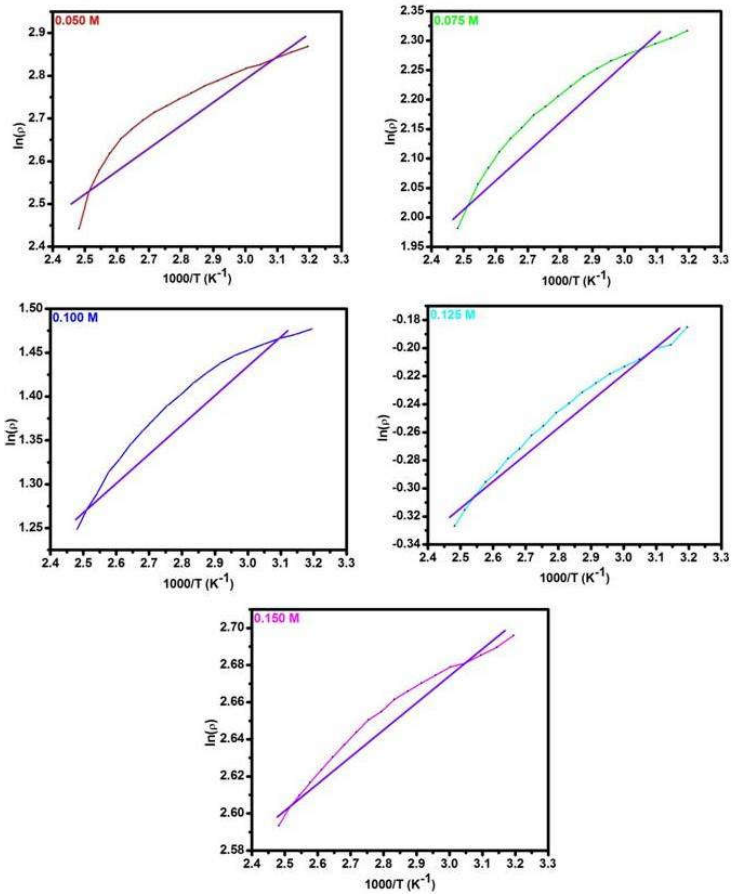

Fig. 9 Arrhenius Plot for SnS thin films for different precursor concentration

IV. CONCLUSION

By nebulized spray pyrolysis technique SnS thin films were prepared at different precursor concentration from 0.050 M to 0.150 M successfully. The obtained SnS thin films were uniform with good adherence and having the orthorhombic structure. The variation in grain size and energy gap by increasing precursor concentration made the samples as an favourable candidate for the applications of optoelectronic device such as photoconductors and solar cells. The high transmittance in the visible region observed at lower precursor concentrations represented the good optical quality of the crystals with the low absorption or scattering losses which lead to the applications particularly as a window layer in solar cells. The optical parameters such as direct band gap energy have been studied in detail. The change in morphology of SnS thin films for different precursor concentration was studied by scanning electron microscope. Energy dispersive X-ray (EDX) pattern confirmed the presence of Sn and S with the chemical stoichiometric. The electrical resistivity of the as-deposited SnS thin films is decreased by increasing the precursor concentration up to 0.125 M and further increased for 0.150 M. The maximum carrier mobility of 23.6 cm^2/Vs was obtained m_c at 0.125M. The optimized condition for the SnS thin films using the nebulized spray pyrolysis technique for the substrate temperature and precursor concentration is 300 ^oC and 0.125 M as confirmed respectively. The investigation results of the SnS thin films grown by nebulized spray pyrolysis technique assure the stability of the film and their employability in solar cell application.

REFERENCES

[1] *R.H. Bube, Photoconductivity of Solids, Wiley, New York, (1960) 233.*

[2] *H. Dittrich, D.J. Vaughan, R.A.D. Pattrick, S. Graeser, M. Lux-Steiner, R. Kunst, D. Lincot, Proceedings of the 13th European PVSEC, Nice, France, (1995) 1299.*

[3] *J.P. Singh, R.K. Bedi, Thin Solid Films 199 (1991) 9.*

[4] *H. Noguchi, A. Setiyadi, H. Tanamura, T. Nagamtomo, O. Omoto, Sol. Energy Mater. Sol. Cells 35 (1994) 325.*

[5] *W. Guang-Pu, Z. Zhi-Lin, Z. Wei-Ming, G. Xiang-Hong, C. Wei Qun, Proceedings of the FWCPEC, Hawaii, U.S.A (1994) 365.*

[6] *A. Ghazali, Z. Zainal, M.Z. Hussein, A. Kassim, Sol. Energy Mater. Sol. Cells 55 (1998) 237.*

[7] *M. Ichimura, L. Takeuchi, Y. Ono, E. Arai, Thin Solid Films 361-362 (2000) 98.*

[8] *L.S. Price, I.P. Parkin, M.A. Field, A.M.E. Hardy, R.J.H. Clark, T.G. Hib- bert, K.C. Molloy, J. Mater. Chem. 10 (2000) 527*

[9] *N.K. Reddy, K.T.R. Reddy, Thin Solid Films 325 (1998) 4.*

[10] *B. Thangaraju, P. Kaliannan, J. Phys. D: Appl. Phys. 33 (2000) 1054.*

[11] *H. Ben Haj Salah, H. Bouzouita, B. Rezig, Thin Solid Films 480 (2005) 439.*

[12] *M. Calixto-Rodriguez, H. Martinez, A. Sanchez-Juarez, J. Campos-Alvarez, A. Tiburcio-Silver, M.E. Calixto, Thin Solid Films 517 (2009) 2497.*

[13] *S. Lopez, S. Granados, A. Ortiz, Semicond. Sci. Technol. 11 (1996) 433.*

[14] *N. Koteeswara Reddy, K.T. Ramakrishna Reddy, Materials Chemistry and Physics 102 (2007) 13.*

[15] *E. Bauer, M.H. Francombe, H. Sato, Single Crystal Films, first ed., Pergamon, London, 1964.*

[16] *A. Khorsand Zak, W.H. A. Majid, M.E. Abrishami, R. Yousefi, Solid State Sci., 13 (2011) 251.*

[17] R.Mariappan, V.Ponnuswamy, P.Suresh, R.Suresh, M.Ragavendar, C.Sankar, Mater. Sci. Semicond. Proc., 16 (2013) 825.
[18] R.Suresh, V.Ponnuswamy, R.Mariappan, N.Senthilkumar, Ceram. Int., 40 (2014) 437.
[19] G.B.Williamson, R.C.Smallman, Philos.Mag., 1 (1956) 34.
[20] M.M.el-Nahass, B.A.Khalifa, H.S.Soliman, M.A.M.Seyam, Thin Solid Films, 515 (2006) 1796.
[21] Chitra Das, Jahanara Begum, Tahmina Begum, Shamima Choudhury, Journal of Bangladesh Academy of Sciences 37 (2013) 83.
[22] A.A. Shama, H.M. Zeyada, Opt. Mater. 24 (2003) 555.
[23] M.M. El-Nahass, H.M. Zeyada, M.S. Aziz, N.A. El-Ghamaz, Opt. Mater. 20 (2002) 159.
[24] P.P. Hankare, A.V. Jadhav, P.A. Chate, K.C. Rathod, P.A. Chavan, S.A. Ingole, J. Alloy. Compd. 463 (2008) 581.
[25] E. Turan, M. Kul, A. Aybek, M. Zor, E. Turan, M. Kul, A. Aybek, M. Zor, J. Phys. D Appl. Phys. 42 (2009) 245408.
[26] A. Akkari, C. Guasch, N. Kamoun-Turki, J. Alloy. Compd. 490 (2010) 180.
[27] E. Guneri, F. Gode, C. Ulutas, F. Kirmizigul, G. Altindemir, C. Gumus, Chalcogenide Lett. 7 (2010) 685.
[28] E. Guneri, C. Ulutas, F. Kirmizigul, G. Altindemir, F. Gode, C. Gumus, Appl. Surf. Sci. 257 (2010) 1189.
[29] A. Kassim, H.S. Min, A. Shariff, M.J. Haron, Res. J. Chem. Environ. 15 (2011) 45.
[30] M. Jayalakshmi, M. Mohan Rao, B.M. Choudary, Electrochem. Commun. 6 (2004) 1119.
[31] N. Sato, M. Ichimura, E. Arai, Y. Yamazaki, Sol. Energy Mater. Sol. Cells 85 (2005) 153.
[32] K.T. Ramakrishna Reddy, P. Prathap, R.W. Miles, Energy Science, Engineering and Technology Nova Science Publishers (2010) 37.
[33] C.D. Lokhande, A.U.Ubale, P.S.Patil, Thin Solid Films, 302 (1997) 1.
[34] R.S.Mane, C.D.Lokhande, Mater. Chem. Phys., 82 (2003) 347.
[35] J.D.Dow, D.Redfield, Phys. Rev., B5 (1972) 594.
[36] P Prathap, YPV Subbaiah, KT Ramakrishna Reddy, J Phys D Appl Phys. 40 (2007) 5275.
[37] N Anitha, M Anitha, J Raj Mohamed, S Valanarasu, L Amalraj, Journal of asian ceramic societies 6 (2018) 121.
[38] Ngamnit Wongcharoen, Thitinai Gaewdang, Materials Science Forum 890 (2017) 295.
[39] A.S. Juarez, A. Ortiz, Semicond. Sci. Technol. 17 (2002) 931.
[40] P.P. Hankare, A.V. Jadhav, P.A. Chate, K.C. Rathod, P.A. Chavan, S.A. Ingole, J. Alloy. Compd. 463 (2008) 581.
[41] S. Lopez, A. Ortiz, Semicond. Sci. Technol. 9 (1994) 2130.